

R. S. Gross (Jet Propulsion Laboratory, California Institute of Technology, Pasadena, CA 91109-8099, USA; [rsg@logos.jpl.nasa.gov](mailto:rsg@logos.jpl.nasa.gov))

A combination of Earth orientation measurements has been generated from space-geodetic observations spanning 1976-1996. The approach taken is the same as that used in generating previous such combinations (e.g., Gross, "Combinations of Earth Orientation Measurements: SPACE94, COMB94, and POLE94", J. Geophys. Res., 101, 8729-8740, 1996) and will be only briefly described here. Since it was desirable to combine only independent measurements, only those series listed in Table 1 were used. Note that only measurements from the Scripps GPS series through May 31, 1992 were used, with measurements from the JPL GPS series EOP(JPL) 95 P 02 used from June 1, 1992 through December 31, 1994, measurements from the IGS combined series EOP(IGS) 95 P 01 used from January 1, 1995 through June 29, 1996, and measurements from the IGS combined series EOP(IGS) 96 P 02 used thereafter. Similarly, only the USNO IRIS Intensive UT1 determinations made after January 1, 1995 were used, with the NOAA IRIS Intensive series being used before then.

Prior to their combination, the bias and rate of each series was iteratively adjusted so as to be in agreement with the bias and rate exhibited by a combination of all other series; the stated uncertainty of each series was adjusted by applying a multiplicative scale factor making the residual of that data, when difference with a combination of all other data, have a reduced chi-square of one; and those data points whose residual values were greater than three times their adjusted uncertainties were deleted. In order for the final combination, SPACE96, to be given within a well-defined terrestrial reference frame, an additional common bias-rate correction was applied to each series so that their combination, SPACE96, would be aligned with the IERS Earth orientation series EOP(IERS) 97 C 04 during 1987-1996. The UT1 values of the entire SPACE96 series have also had the new 9.3- and 18.6-year terms included by adding the correction:

$$UT1_{new} - UT1_{old} = -0.176 \sin(\Omega) - 0.0042 \sin(2 \cdot \Omega) \text{ (ins)}$$
which is consistent with the new GST definition (see IERS Conventions (1996), pp. 21-22), but is of opposite sign to the correction given in IERS Gazette No. 8. The total bias-rate corrections and uncertainty scale factors that have been applied to the individual series prior to their combination into SPACE96 are given in Table 1 in the natural reference frame for each data type: the transverse (T), vertical (V) frame for single baseline VLBI measurements; the variation-of-latitude (VOL), UTO frame for single station LLR measurements; and the usual UTPM (PMX, PMY, UT1) frame for all other measurements. The uncertainties in the bias-rate corrections (given in parentheses in Table 1) are the formal errors in determining the incremental bias-rate corrections during the last iteration.

ACKNOWLEDGMENTS . The work described here was performed at the Jet Propulsion Laboratory, California Institute of Technology, under contract with the National Aeronautics and Space Administration.

TABLE 1. ADJUSTMENTS TO DATA SETS PRIOR TO COMBINATION

DATA SET NAME	BIAS (mas)		RATE (mas/yr)		UNCERTAINTY SCALE FACTOR				
LLR (JPL; 04FEB97)	VOL	UTO	VOL	UTO	VOL	UTO			
McDonald Cluster	0.209 (0.121)	-0.336 (0.107)	-0.028 (0.041)	-0.112 (0.035)	1.458	1.209			
CERGA	0.258 (0.057)	-0.008 (0.038)	0.132 (0.021)	-0.003 (0.014)	1.828	1.349			
Haleakala	0.942 (1.146)	-1.518 (0.715)	-0.126 (0.231)	-0.121 (0.152)	2.015	1.703			
DSN (JPL; 96R01)	T	v	T	V	T	V			
CA-Spain Cluster	-0.452 (0.027)	0.490 (0.063)	0.117 (0.012)	0.165 (0.028)	1.348	1.102			
CA-Australia Cluster	1.153 (0.021)	-0.117 (0.059)	0.047 (0.008)	0.037 (0.024)	1.392	1.115			
NASA SGP (GLB1057c)	T	V	T	V	T	V			
Westford-Ft. Davis	8.370 (3.758)	4.775 (6.301)	0.830 (0.378)	0.477 (0.630)	1.304	0.837			
Westford-Mojave	0.432 (0.232)	-0.077 (0.428)	0.121	-0.050	2.564	0.858			
NASASGP(1057C)	PMX	PMY	UT1	PMX	PMY	UT1	PMX	PMY	UT1
Multi-baseline	-1.024 (0.013)	-1.331 (0.011)	0.008 (0.018)	-0.073 (0.005)	0.026 (0.004)	-0.063 (0.007)	1.586	1.428	1.687
NOAA (95R02)	PMX	PMY	UT1	PMX	PMY	UT1	PMX	PMY	UT1
IRIS Inten.	---	---	0.296 (0.021)	---	---	-0.013 (0.006)	---	---	0.934
USNO (19FEB97)	PMX	PMY	UT1	PMX	PMY	UT1	PMX	PMY	UT1
IRIS Inten.	---	---	-1.004 (0.044)	---	---	0.084 (0.018)	---	---	1.048
UTCSR (96L01)	PMX	PMY	UT1	PMX	PMY	UT1	PMX	PMY	UT1
LAGEOS SLR	-0.047 (0.014)	0.792 (0.011)	---	0.053 (0.004;	0.109 (0.004)	---	0.982	0.835	---
GPS (SIO93P01)	PMX	PMY	UT1	PMX	PMY	UT1	PMX	PMY	UT1
Scripps	-0.968 (0.034)	-0.716 (0.039)	---	0.129	0.100	---	1.879	1.932	---
GPS (JPL95P02)	PMX	PMY	UT1	PMX	PMY	UT1	PMX	PMY	UT1
JPL	-0.100 (0.024)	0.512 (0.022)	---	0.110 (0.020,	-0.067 (0.018:	---	3.007	2.677	---
GPS (IGS95P01)	PMX	PMY	UT1	PMX	PMY	UT1	PMX	PMY	UT1
IGS	0.175 (0.086)	<b>0.412</b> (0.068)	---	0.145 (0.031'	0.241 (0.025)	---	2.578	1.424	---
GPS (IGS96P02)	PMX	PMY	UT1	PMX	PMY	UT1	PMX	PMY	UT1
IGS	-0.887 (0.025)	-0.477 (0.016)	---	0.129	0.100	---	3.591	1.060	---

REFERENCE DATE FOR BIAS-RATE ADJUSTMENT IS 1993.0

Technical description of solution JPL 97 C 01

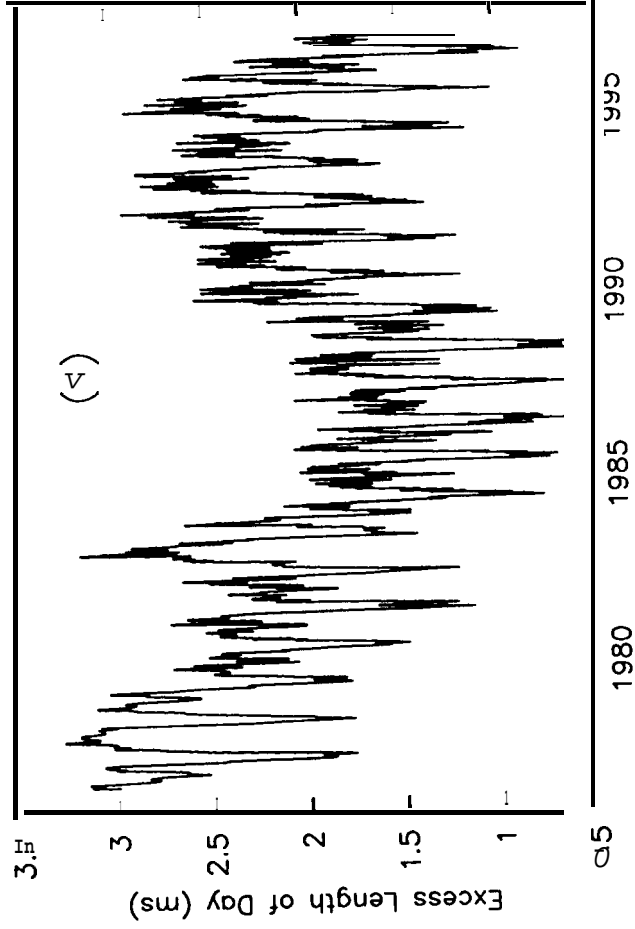
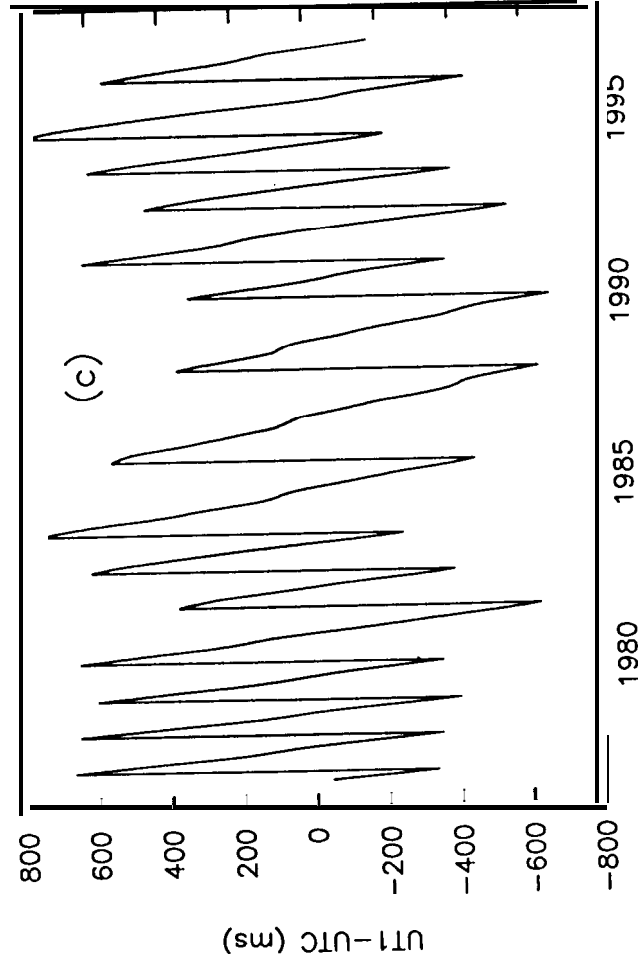
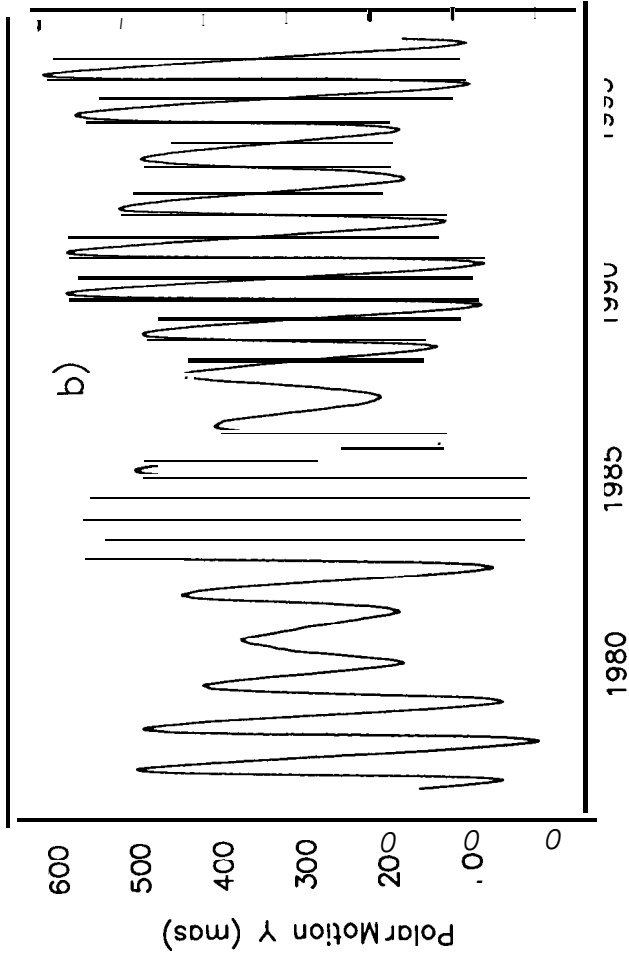
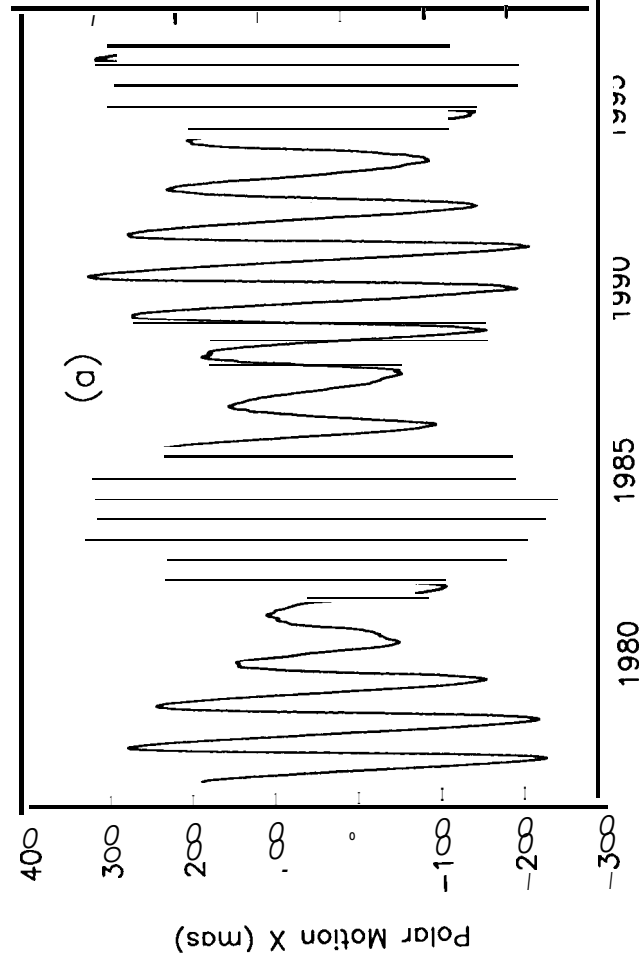
- 1 - Technique: Combined
- 2 - Analysis Center: Jet Propulsion Laboratory
- 3 - Software used: **Kalman** Earth Orientation Filter (KEOF) OP-B
- 4 - Data span: Ott 76 - Feb 97 at 1-day intervals
- 5 - Celestial Reference Frame: Not Applicable
  - a - Nature:
  - b - Definition of the orientation:
- 6 - Terrestrial Reference Frame: Not Applicable
  - a - Relativity **scale**:
  - b - Velocity of light:
  - c - Geogravitational constant:
  - d - Permanent tidal correction:
  - e - Definition of the origin:
  - f - Definition of the orientation:
  - g - Reference epoch:
  - h - Tectonic plate model:
  - i - **Constraint for time evolution**:
- 7 - **Earth orientation**: EOP(JPL) 97 C 01
  - a - A priori precession model: Not Applicable
  - b - A priori nutation model: Not Applicable
  - c - Short-period tidal variations in x, y, UT1:  
  
When necessary, diurnal and **semidiurnal** tidal variations have been removed from the individual EOP series prior to their combination into EOP(JPL) 97 C 01. Diurnal and **semidiurnal** tidal terms have not been added back and are therefore not included in the values reported in EOP(JPL) 97 C 01.
- 8 - Estimated Parameters:
  - a - Celestial Frame:
  - b - **Terrestrial Frame**:
  - c - Earth Orientation: **PMX, PMY, UT1-UTC**
  - d - Others:

MJD	PMX (arc see)	PMY (arc see)	UT1 -UTC (see)	SIG X (arc see)	SIG Y (arc see)	SIG U (see)	COR XY	COR XV	COR YU			
43049.000	0.1882687	0.1619289	-0.0435872	0 0	0.0044677	0.0030681	0.0006662	0 0 0	-0.0063	0.2081	0.10?0	0 0 0
43050.000	0.1877425	0.1598036	-0.0467965	0 0	0.0041895	0.0029587	0.0006283	0 0 0	-0.0209	0.1969	0.1261	0 0 0
43051.000	0.1872142	0.1576080	-0.0499560	0 0	0.0039636	0.0028638	0.0005842	0 0 0	-0.0309	0.1917	0.1490	0 0 0
43052.000	0.1866756	0.1553541	-0.0531267	0 0	0.0037853	0.0027808	0.0005352	0 0 0	-0.0365	0.1934	0.1753	0 0 0
43053.000	0.1861189	0.1530543	-0.0563531	0 0	0.0036490	0.0027079	0.0004828	0 0 0	-0.0381	0.2034	0.2042	0 0 0
43054.000	0.1855346	0.1507246	-0.0596580	0 0	0.0035484	0.0026442	0.0004293	0 0 0	-0.0370	0.2231	0.2343	0 0 0
43055.000	0.1849101	0.1483876	-0.0630439	0 0	0.0034760	0.0025894	0.0003774	0 0 0	-0.0345	0.2536	0.2623	0 0 0
43056.000	0.1842329	0.1460667	-0.0664959	0 0	0.0034252	0.0025448	0.0003311	0 0 0	-0.0322	0.2945	0.2817	0 0 0
43057.000	0.1834909	0.1437831	-0.0699840	0 0	0.0033907	0.0025130	0.0002942	0 0 0	-0.0312	0.3423	0.2836	0 0 0
43058.000	0.1826700	0.1415423	-0.0734610	0 0	0.0033687	0.0024966	0.0002670	0 0 0	-0.0324	0.3927	0.2646	0 0 0
43059.000	0.1817593	0.1393406	-0.0768810	0 0	0.0033565	0.0024980	0.0002484	0 0 0	-0.0360	0.4409	0.2273	0 0 0
43060.000	0.1807553	0.1371720	-0.0802118	0 0	0.0033510	0.0025163	0.0002378	0 0 0	-0.0418	0.4809	0.1786	0 0 0
43061.000	0.1796575	0.1350323	-0.0834358	0 0	0.0033490	0.0025487	0.0002374	0 0 0	-0.0493	0.5005	0.1268	0 0 0
43062.000	0.1784682	0.1329134	-0.0865518	0 0	0.0033486	0.0025926	0.0002510	0 0 0	-0.0577	0.4876	0.0795	0 0 0
43063.000	0.1771951	0.1308046	-0.0895799	0 0	0.0033488	0.0026456	0.0002808	0 0 0	-0.0659	0.4442	0.0422	0 0 0
43064.000	0.1758467	0.1287028	-0.0925541	0 0	0.0033485	0.0027039	0.0003251	0 0 0	-0.0734	0.3867	0.0164	0 0 0
43065.000	0.1744284	0.1266138	-0.0955133	0 0	0.0033460	0.0027622	0.0003787	0 0 0	-0.0800	0.3306	0.0001	0 0 0
43066.000	0.1729436	0.1245436	-0.0985009	0 0	0.0033404	0.0028164	0.0004363	0 0 0	-0.0858	0.2828	-0.0099	0 0 0
43067.000	0.1713957	0.1224979	-0.1015650	0 0	0.0033318	0.0028638	0.0004938	0 0 0	-0.0907	0.2439	-0.0162	0 0 0
43068.000	0.1697869	0.1204830	-0.1047530	0 0	0.0033204	0.0029025	0.0005486	0 0 0	-0.0949	0.2127	-0.0204	0 0 0
43069.000	0.1681156	0.1185069	-0.1081043	0 0	0.0033054	0.0029312	0.0005988	0 0 0	-0.0983	0.1878	-0.0236	0 0 0
43070.000	0.1663795	0.1165781	-0.1116393	0 0	0.0032864	0.0029493	0.0006427	0 0 0	-0.1008	0.1681	-0.0262	0 0 0
43071.000	0.1645764	0.1147050	-0.1153476	0 0	0.0032638	0.0029574	0.0006795	0 0 0	-0.1022	0.1528	-0.0286	0 0 0
43072.000	0.1627046	0.1128956	-0.1191803	0 0	0.0032385	0.0029566	0.0007083	0 0 0	-0.1022	0.1412	-0.0311	0 0 0
43073.000	0.1607635	0.1111526	-0.1230545	0 0	0.0032105	0.0029468	0.0007284	0 0 0	-0.1009	0.1329	-0.0338	0 0 0
43074.000	0.1587531	0.1094744	-0.1268742	0 0	0.0031796	0.0029271	0.0007396	0 0 0	-0.0984	0.1276	-0.0367	0 0 0
43075.000	0.1566734	0.1078589	-0.1305606	0 0	0.0031459	0.0028974	0.0007415	0 0 0	-0.0946	0.1251	-0.0400	0 0 0
43076.000	0.1545232	0.1062997	-0.1340786	0 0	0.0031091	0.0028576	0.0007340	0 0 0	-0.0902	0.1255	-0.0437	0 0 0
43077.000	0.1523005	0.1047886	-0.1374445	0 0	0.0030691	0.0028081	0.0007173	0 0 0	-0.0856	0.1288	-0.0479	0 0 0
43078.000	0.1500035	0.1033173	-0.1407123	0 0	0.0030262	0.0027501	0.0006916	0 0 0	-0.0815	0.1350	-0.0524	0 0 0

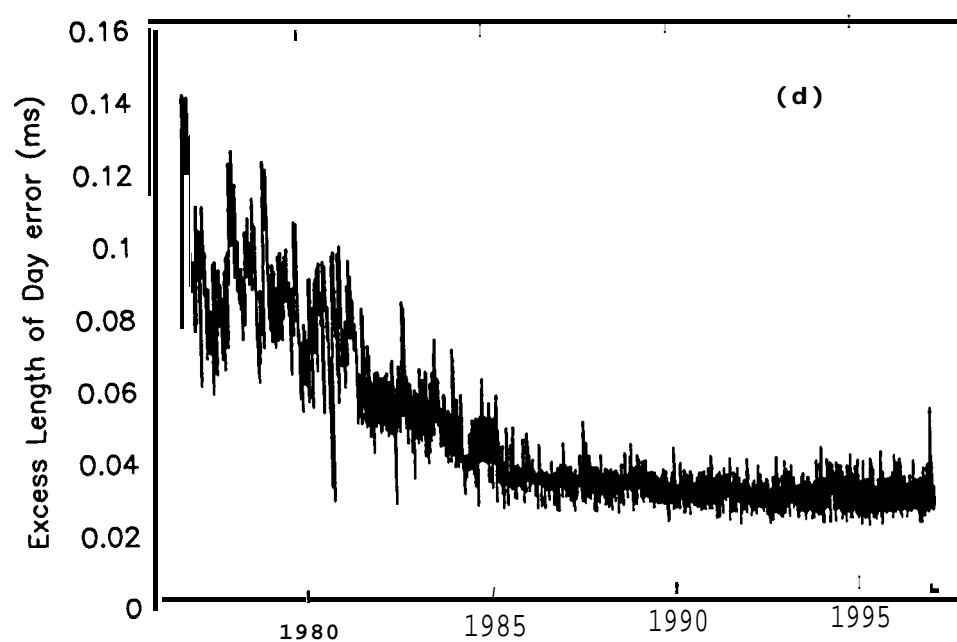
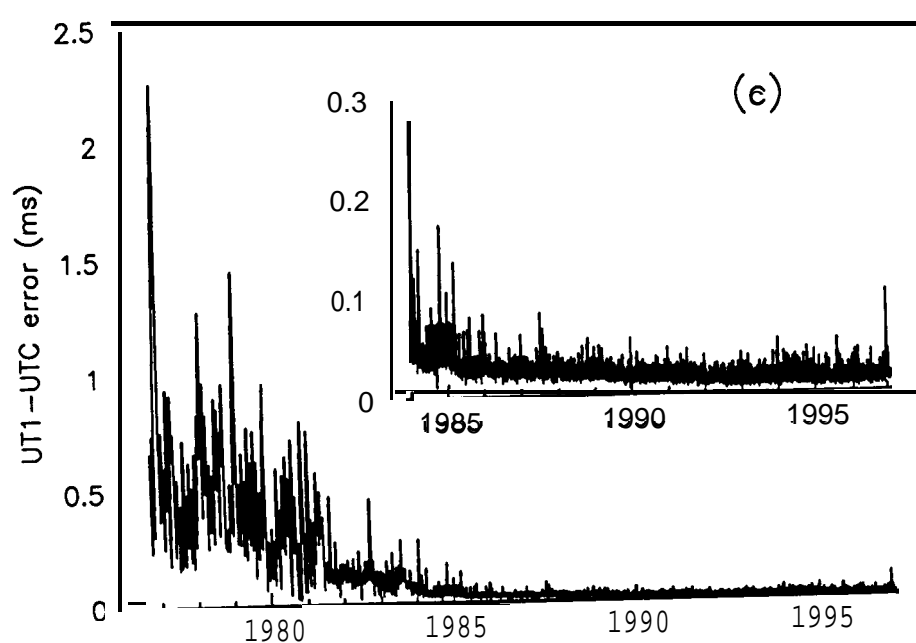
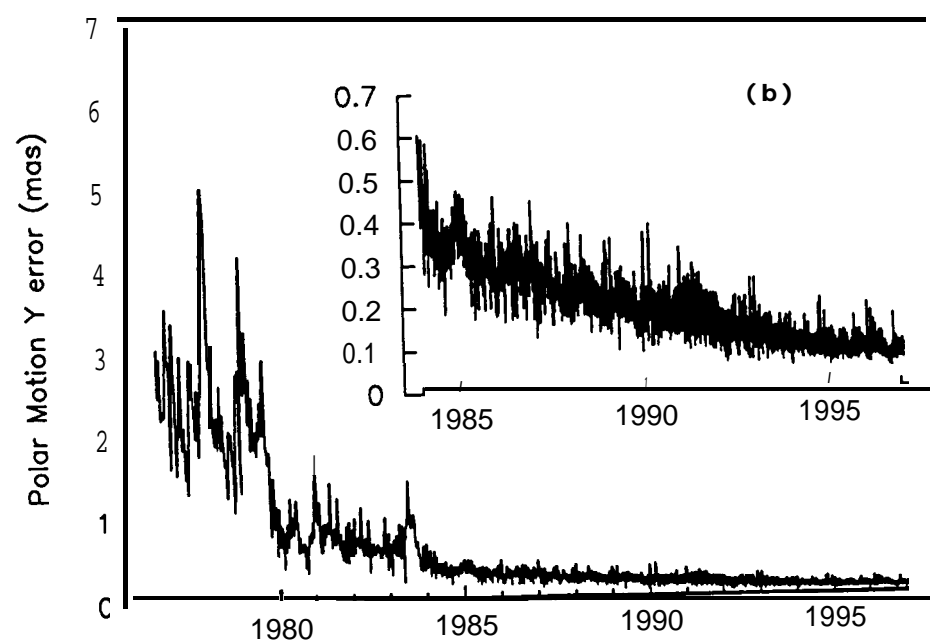
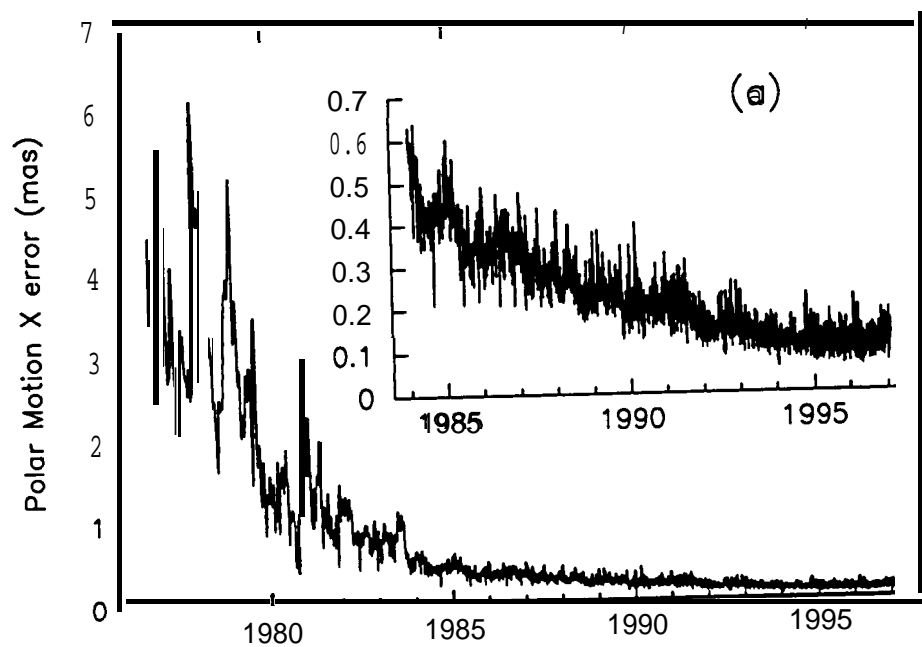
7379 records not shown

50458.000	-0.0533266	0.1059693	-0.1283603	0 0	0.0000746	0.0000967	0.0000287	0 0 0	0.0027	-0.0002	-0.0002	0 0 0
50459.000	-0.0562117	0.1071397	-0.1304272	0 0	0.0000743	0.0000796	0.0000253	0 0 0	0.0003	-0.0023	0.0017	0 0 0
50460.000	-0.0590361	0.1083565	-0.1326017	0 0	0.0000904	0.0000761	0.0000177	0 0 0	0.0097	-0.0809	0.0282	0 0 0
50461.000	-0.0616546	0.1096634	-0.1348062	0 0	0.0001495	0.0000891	0.0000236	0 0 0	0.0066	-0.0496	0.0151	0 0 0
50462.000	-0.0639989	0.1111015	-0.1370169	0 0	0.0001834	0.0000916	0.0000274	0 0 0	0.0013	-0.0058	0.0002	0 0 0
50463.000	-0.0661122	0.1127617	-0.1392110	0 0	0.0001925	0.0000963	0.0000352	0 0 0	-0.0039	0.0047	-0.0049	0 0 0
50464.000	-0.0680877	0.1146437	-0.1413328	0 0	0.0001783	0.0000866	0.0000237	0 0 0	-0.0040	0.0064	-0.0070	0 0 0
50465.000	-0.0700256	0.1166575	-0.1433385	0 0	0.0001676	0.0000695	0.0000099	0 0 0	-0.0007	-0.0024	0.0002	0 0 0
50466.000	-0.0720566	0.1186733	-0.1451684	0 0	0.0001532	0.0000717	0.0000103	0 0 0	0.0043	-0.0348	0.0080	0 0 0
50467.000	-0.0743312	0.1206826	-0.1468194	0 0	0.0001346	0.0000829	0.0000099	0 0 0	0.0021	-0.0018	0.0004	0 0 0
50468.000	-0.0769295	0.1227532	-0.1483547	0 0	0.0001231	0.0000810	0.0000175	0 0 0	0.0001	0.0019	-0.0002	0 0 0
50469.000	-0.0797434	0.1248415	-0.1498013	0 0	0.0000996	0.0000890	0.0000105	0 0 0	-0.0043	-0.0001	-0.0002	0 0 0
50470.000	-0.0825169	0.1268696	-0.1512187	0 0	0.0000991	0.0001102	0.0000120	0 0 0	-0.0069	0.0038	0.0022	0 0 0
50471.000	-0.0851783	0.1287574	-0.1526687	0 0	0.0000985	0.0001100	0.0000183	0 0 0	-0.0084	0.0041	0.0023	0 0 0
50472.000	-0.0878441	0.1305560	-0.1541367	0 0	0.0000881	0.0001028	0.0000109	0 0 0	-0.0003	0.0001	0.0001	0 0 0
50473.000	-0.0906574	0.1323220	-0.1556223	0 0	0.0000970	0.0001016	0.0000102	0 0 0	0.0009	0.0000	0.0000	0 0 0
50474.000	-0.0936832	0.1340412	-0.1571365	0 0	0.0001153	0.0000937	0.0000094	0 0 0	0.0029	0.0000	0.0000	0 0 0
50475.000	-0.0967840	0.1358116	-0.1586943	0 0	0.0001475	0.0000850	0.0000168	0 0 0	0.0024	0.0000	0.0000	0 0 0
50476.000	-0.0998306	0.1376938	-0.1603377	0 0	0.0001653	0.0000756	0.0000105	0 0 0	0.0013	0.0000	0.0000	0 0 0
50477.000	-0.1028078	0.1395880	-0.1620104	0 0	0.0001660	0.0000746	0.0000148	0 0 0	-0.0006	0.0000	0.0000	0 0 0
50478.000	-0.1057231	0.1414381	-0.1636029	0 0	0.0001637	0.0000744	0.0000177	0 0 0	0.0007	0.0000	0.0000	0 0 0
50479.000	-0.1086139	0.1434542	-0.1651593	0 0	0.0001484	0.0000662	0.0000102	0 0 0	-0.0010	0.0000	0.0000	0 0 0
50480.000	-0.1115322	0.1456679	-0.1666617	0 0	0.0001258	0.0000716	0.0000116	0 0 0	-0.0017	0.0000	0.0000	0 0 0
50481.000	-0.1144556	0.1478780	-0.1680372	0 0	0.0001174	0.0000816	0.0000098	0 0 0	-0.0001	0.0000	0.0000	0 0 0
50482.000	-0.1172880	0.1500344	-0.1693282	0 0	0.0001268	0.0000684	0.0000168	0 0 0	0.0026	0.0000	0.0000	0 0 0
50483.000	-0.1199702	0.1522912	-0.1705886	0 0	0.0001399	0.0000731	0.0000109	0 0 0	-0.0018	0.0000	0.0000	0 0 0
50484.000	-0.1224708	0.1546974	-0.1718991	0 0	0.0001551	0.0000916	0.0000166	0 0 0	0.0010	0.0000	0.0000	0 0 0
50485.000	-0.1247500	0.1571103	-0.1733433	0 0	0.0001559	0.0000924	0.0000187	0 0 0	-0.0016	0.0000	0.0000	0 0 0
50486.000	-0.1267743	0.1594872	-0.1749582	0 0	0.0001384	0.0001016	0.0000115	0 0 0	-0.0018	0.0000	0.0000	0 0 0
50487.000	-0.1285962	0.1618867	-0.1767785	0 0	0.0001323	0.0000993	0.0000123	0 0 0	0.0003	0.0000	0.0000	0 0 0

# COMBINED EARTH ORIENTATION SERIES: SPACE96



# COMBINED EARTH ORIENTATION SERIES: SPACE96



JET PROPULSION LABORATORY

NOTIFICATION OF CLEARANCE

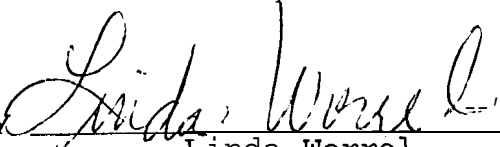
04/17/97

TO: R. Goldstein  
FROM : Logistics and Technical Information Division  
SUBJECT: Notification of Clearance - CL 97-0440

The following title has been cleared by the Document Review Services, Section 644, for public release, presentation, and/or printing in the open literature:

Radar Observations of Space Debris

This clearance is issued for the full paper and is valid only for release in the U.S.

Clearance issued by   
Linda Worrel  
Document Review Services  
Section 644

(Over)

Senior JPL Author, - RICHARD GOLDSTEIN	Section 330	Mail Stop 300-227	Ext. 4-6999	Due Date
---	----------------	----------------------	----------------	----------

**COMPLETE TITLE**  
RADAR OBSERVATIONS OF SPACE DEBRIS

Foreign  Domestic Account Code \_\_\_\_\_  Premeeting publication  
 ABSTRACT (including extended abstract)  Publication on meeting day  
 FULL PAPER (including viewgraphs, poster, videocassette)  Postmeeting publication  
 Journal Name ICARUS  Poster session  
 Meeting - Subject \_\_\_\_\_  Oral presentation  
 Sponsoring Society \_\_\_\_\_  
 Meeting Date \_\_\_\_\_ Location \_\_\_\_\_

BOOK OR BOOK CHAPTER DR: 4/4/97  
 Assigned Laboratory Task OR  Private Venture

PUBLICATION  BROCHURE  NEWSLETTER  For release on the Internet • I within JPL  
 • I outside of NASA

URL: \_\_\_\_\_ FTP: \_\_\_\_\_

Was previously cleared: Clearance No(s):  
 CL- \_\_\_\_\_ Date \_\_\_\_\_ Author(s) \_\_\_\_\_  
 CL- \_\_\_\_\_ Date \_\_\_\_\_ Author(s) \_\_\_\_\_

**REPORTABLE INFORMATION**

THIS WORK:  New technology not previously reported  
 Nature of this work (please describe) \_\_\_\_\_

Covers work previously reported in New Technology Report (NTR) No. \_\_\_\_\_  
 Provides more information for earlier NTR No(s). \_\_\_\_\_

**FOR TECHNOLOGY REPORTING AND COMMUNICATIONS USE ONLY**

Release  Ex Post Facto  Release Delayed or Conditional

Comments:

**FOR SECTION 644 USE ONLY** *SP1115*

Editor \_\_\_\_\_ Ext. \_\_\_\_\_ Document No. \_\_\_\_\_  
 Customer Code (RTOP No.) \_\_\_\_\_ Group \_\_\_\_\_ Condition \_\_\_\_\_

**AUTHORIZATION** (please use blue ink)  
 The signatory in this column attests to the technical accuracy of the subject document.

<i>Richard Goldstein</i>	4/3/97	Technology Reporting and Communications Date <i>Linda Worell</i> 4/17/97 Document Reviewer Date
Senior JPL Author	Date	
<i>[Signature]</i>	4/3/97	
Manager/Supervisor or equivalent	Date	
Print Name and Title of Manager/Supervisor		

NOTE: All full papers and Internet URLs require Section or Project Manager approval. All abstracts require Group Supervisor approval only.



20430  
R 17  
AUTHORIZATION FOR THE EXTERNAL RELEASE OF INFORMATION

Submit URL (if applicable) or two copies of the abstract or full paper to Document Review, 111-120

CL No.

(for DRS use only)

Senior JPL Author <u>RICHARD GOLDSTEIN</u>	Section <u>330</u>	Mail Stop <u>300-227</u>	Ext. <u>4-6999</u>	Due Date
---	-----------------------	-----------------------------	-----------------------	----------

**COMPLETE TITLE**  
RADAR OBSERVATIONS OF SPACE DEBRIS

Foreign  Domestic Account Code \_\_\_\_\_  Premeeting publication

ABSTRACT (including extended abstract) **DRS: 4/4/97**  Publication on meeting day

FULL PAPER (including viewgraphs, poster, videocassette)  Postmeeting publication

Journal Name ICARUS  Poster session

Meeting - Subject \_\_\_\_\_  Oral presentation

Sponsoring Society \_\_\_\_\_ **RECEIVED**

Meeting Date \_\_\_\_\_ Location \_\_\_\_\_ **APR - 4 1997**

BOOK OR BOOK CHAPTER JPL TU OFFICE

Assigned Laboratory Task OR  Private Venture

PUBLICATION  BROCHURE  Newsletter  For release on the Internet • I within JPL  
• I outside of NASA

URL: \_\_\_\_\_ FTP: \_\_\_\_\_

Was previously cleared: Clearance No(s):

CL- \_\_\_\_\_ Date \_\_\_\_\_ Author(s) \_\_\_\_\_

CL- \_\_\_\_\_ Date \_\_\_\_\_ Author(s) \_\_\_\_\_

**Reportable INFORMATION**

THIS WORK:  New technology not previously reported

Nature of this work (please describe) \_\_\_\_\_

Covers work previously reported in New Technology Report (NTR) No. \_\_\_\_\_

Provides more information for earlier NTR No(s). \_\_\_\_\_

**'OR TECHNOLOGY REPORTING AND COMMUNICATIONS USE ONLY**

Release  Ex Post Facto  Release Delayed or Conditional

Comments: \_\_\_\_\_

**'OR SECTION 644 USE ONLY**

Editor \_\_\_\_\_ Ext. \_\_\_\_\_ Document No. \_\_\_\_\_

Customer Code (RTOP No.) \_\_\_\_\_ Group \_\_\_\_\_ Condition \_\_\_\_\_

**AUTHORIZATION** (please use blue ink)

The signatory in this column attests to the technical accuracy of the subject document.

Richard Goldstein 4/3/97  
Senior JPL Author Date

[Signature] 4/3/97  
Manager/Supervisor or equivalent Date

[Signature] 4/11/97  
Technology Reporting and Communications Date

Print Name and Title of Manager/Supervisor

NOTE: All full papers and Internet URLs require Section or Project Manager approval.  
All abstracts require Group Supervisor approval only.

Document Reviewer \_\_\_\_\_ Date \_\_\_\_\_

## RADAR OBSERVATIONS OF SPACE DEBRIS

R. M. Goldstein  
Jet Propulsion Laboratory, California Institute of Technology  
4800 Oak Grove Dr., Pasadena, CA 91109  
Phone: 818 354-6999  
E-mail : goldstein@kahuna.jpl.nasa.gov

S. J. Goldstein, Jr.  
University of Virginia

and

D. J. Kessler  
Orbital Debris and Meteoroid Consultant  
Lockheed Martin Engineering and Science

April 2, 1997

### ABSTRACT

Radar monitoring of small particles of orbital debris at NASA's Goldstone Tracking Station has resulted in the detection of 1124 objects in 38.4 hours of observations. Many of the objects orbit in clusters; the largest appears to be remnants of the West Ford Needles, launched 3 decades earlier.

#### 1. Introduction

~~Orbiting~~ Orbiting debris is recognized as a present and growing hazard for both humans and machines in space. Space collisions can have a closing velocity of  $15 \text{ km s}^{-1}$ , and even small particles are a serious safety concern. Knowledge of the changing environment of debris is necessary for both space mission design and for the assessment of debris mitigation policies.

Currently, the United States Space Command, Johnson (1993), maintains a catalog of orbital elements of space objects larger than about 10 cm. Monitoring of the flux of smaller objects has been accomplished by routine ground-based optical, Potter (1995), and radar observations, Stansbery, *et al* (1993). Very small particles of orbiting debris have also been detected by *in situ* spacecraft, Mandeville and Berthaud (1995), which have subsequently returned to Earth.

Occasionally, a 3.5 cm radar at NASA's Goldstone tracking station is available for orbital debris observations. This powerful radar which can detect a 3 mm conducting sphere orbiting at an altitude of 1000 km, helps to fill an observational gap in the on-going debris survey, Goldstein and Randolph (1992) and Goldstein and Goldstein (1994 and 1995).

## 2. Observations

We report here the results of the Goldstone observations for seven runs between October, 1994, and March, 1996. The radar configuration was the same as reported previously, except that the maximum range was extended to 3200 km by increasing the listening period between transmitted pulses.

Each transmitted pulse (51 kHz up-chirps alternated with down-chirps) lasted for 2.3 ms and was followed by 0.2 ms of dead time and 20 ms of receive time. This arrangement permits the separate measurement of range and range-rate, provided that only one object at a time is in the beam.

A typical particle of orbital debris at 1200 km altitude remains in the radar half-power beam for about 90 ms, thereby experiencing 4 pulses of illumination. No attempt was made to track the particles; the antennas were not moved.

Two antennas were used; a 70 m dish for the transmitter, and a 35 m dish for the receiver. These antennas are spaced 497 meters along a line bearing 154.6 degrees from north. The larger, transmitting antenna was aimed 1.50 degrees from the zenith, towards the back of the receiving antenna. The receiving antenna, which could maintain pointing accuracy closer to the zenith, was aimed 1.44 degrees from the zenith, and along the same azimuth. The geometry for the pointing is given in figure 1, where the lower beam half-power intersection is shown at 280 km altitude, and the upper intersection at about 3000 km. The location of the upper intersection is a very sensitive function of antenna pointing.

As can be seen, the capture cross-section of the radar is a function of range and direction of the debris motion. Additionally, larger particles that do not cross the beam intersection can be detected through the antenna sidelobes. Such particles can be identified because they produce echoes over a longer time interval than the nominal duration of a main-beam crossing.

The observations are summarized in Table I:

Table I

Date	Hours, GMT	Hits
Ott 17, 1994	7.384 - 10.969	119
Ott 24, 1994	3.593 - 10.407	292
Nov 4, 1994	5.784 - 12.978	194
Dec 5, 1994	3.002 - 8.583	135
Nov 13, 1995	8.037 - 13.860	174
Nov 14, 1995	9.238 - 10.923	59
Mar 11, 1996	22.349 - 6.105	151

### 3. Data

There were 1124 detections over the 38.4 hours. A detection is defined as a threshold crossing on both the up- and down-chirp responses. The threshold was chosen such that noise alone could produce a false detection on an average of once per 28 hours.

Figure 2 shows the system response to a detection that was 1.4 times the threshold. Range is plotted as the abscissa. The curves are paired; the first of each pair is the result for two up-chirps, the second for two down-chirps. Each pair represents successive 90 ms steps of time. The true range of the object is estimated as the average of the up- and down-chirp apparent ranges; the range rate is proportional to their difference.

The detection shown in this figure is likely to have been from a particle crossing the main beam. However, 65 of the observed events appeared on too many of the curves for their measured ranges. These have been deemed side-lobe crossings, and have been removed from the data set.

Figure 3 presents the main-beam cumulative results, where particle effective diameter is plotted as a function of range. Effective diameter is defined as the diameter of a conducting sphere which would return the same power, at the same distance, as was actually measured.

The particles were assumed to pass through the center of the main antenna beam, and the measured power was corrected for the pattern of the smaller antenna. Effective diameter is computed from the measured radar cross section according to either the geometric cross section for larger particles or the Rayleigh approximation for small particles.

$$\sigma = \frac{\pi d^2}{4}, \text{ for larger particles} \quad (1a)$$

$$\sigma = \frac{d^6 \pi^5}{\lambda^4}, \text{ for smaller particles,} \quad (1b)$$

where  $\sigma$  is the radar cross section,  $\lambda$  is the wavelength and  $d$  is the effective diameter.

The lower limit seen in figure 3 is the result of the echo power being below the detection threshold; there appears to be a genuine lack of larger particles at the lower altitudes.

Figure 4 presents the line-of-sight velocity, as a function of range, for the main-beam detections. Positive velocities are for approaching particles. The system bandwidth permitted detection of particles with line-of-sight velocities between  $\pm 810 \text{ m s}^{-1}$ . Any particles with greater velocity have been filtered out by the detection system. A velocity of half of that limit would cause half of the received energy to be lost. A

correction has been made to the radar cross section for this effect .

The Goldstone radar normally transmits right-hand circular polarization and receives the opposite sense. During one hour, when the detection rate was high, the receiver polarization was reversed. The effects of this change will be noted subsequently.

#### 4. Flux

All of the data were sorted into 100 km altitude bins and normalized by the main-beam geometric cross section (i. e., the area shown in figure 1) , and by the number of days of observation. The resulting flux measurements are given in figure 5. Most, but not all, of the flux of Figure 5 represents objects in the millimetric range.

There is a peak in the flux histogram near 900 km. It has been previously observed by the Haystack, Stansbery *et al* (1995), and Goldstone, Goldstein and Goldstein (1995), radars. There is a second peak near 2900 km, not previously reported in radar measurements from the ground.

Figures 3, 4 and 5 show that much of the space debris population exists in range and radial-velocity clusters, which suggests common origins for them. We will discuss possible origins for both clusters in the following sections.

#### 5. Near Cluster

The two clusters of points at ranges between 740 and 1020 km, shown in figure 4, appear to be observations of the same family of objects, seen once on the ascending portion of their orbits, and seen again on the descending portion.

Under the one-family, circular orbit assumptions, we can calculate the inclination of the orbits from the velocity ratio of the clusters. The velocities are projections, as follows:

$$v_1 \propto -\cos(\beta-\alpha); \quad \textit{ascending} \quad (2a)$$

$$v_2 \propto +\cos(\beta+\alpha); \quad \textit{descending} \quad (2b)$$

where  $\alpha$  is the azimuth of the ascending pass, and  $\beta$  is the pointing azimuth of the antennas.

The circular orbit assumption is strengthened by the high concentration of particles, as shown in figure 5. Only circular orbits can maintain this density of objects in such a narrow altitude band.

The orbital inclination is then determined by the solution for  $\alpha$  and the known station latitude, with a small correction to  $\alpha$  occasioned by the rotation of the Earth. The resulting

inclination is  $70 \pm 5$  degrees. The uncertainty is estimated from the spread within the clusters. For a polar orbit, the two velocity clusters would coalesce. For an inclination greater than 90 degrees, the magnitude of the receding cluster velocity would be less than that of the approaching one.

During our hour-long experiment on polarization reversal, the detection rate for particles in the 740 to 1020 km altitude range dropped to 4 events per hour from an average of 10.8 events per hour.

Stansberry, et al (1995), and Kessler, et al (1995), have discussed radar observations at 3 cm for altitudes between 850 and 1000 km. They calculated an average orbital inclination of 65 deg, and referred to observations at Haystack that show that the particles do not reflect the orthogonal circular polarization. They concluded that the particles are spheres with diameters between 0.6 and 2 cm and that 70,000 are in orbit. These data led them to identify the source of the near cluster particles as the RORSAT satellite family. These satellites use a mixture of sodium and potassium in liquid form to cool their nuclear power supplies. Stansberry, et al (1995), adopt the hypothesis that the coolant leaks to form the spherical particles.

Our measurements show that the clustering in altitude near 900 km extends to particles at least as small as 0.25 cm diameter. The calculation of orbital inclination above is in agreement with that of Stansberry, et al (1995). Our data leads to an additional population of 500,000 particles with diameters between 0.25 and 0.6 cm.

## 6. Distant Cluster

These particles, seen in figures 3 and 4, have radar cross sections from  $27 \text{ mm}^2$  at detection threshold, to a maximum observed of  $466 \text{ mm}^2$ . They cluster in the altitude range between 2500 and 3100 km. They also show a marked clustering in time, which we show as histograms in figure 6. No statistical effect was noted for these particles during the hour of polarization reversal. Such a result is to be expected if the objects are wires. We estimate that there are 40,000 of these particles in orbit.

### 6a. Average Orbital Constants

Previously, Goldstein and Goldstein (1994, 1995), we have found average semi-major axes and eccentricities for groups of space-debris particles from least-square analysis of observed ranges and Doppler shifts at the zenith. The present observations, however, were made 1.5 degrees away from the zenith. The measured range no longer adds directly to the geocentric radius to give the orbital radius, and the Doppler shift is not just the time derivative of the orbital radius for it now contains a small component of the orbital velocity.

However, we have found two long runs of observations where the Doppler shifts were nearly all of the same sense. One group with inward motion is listed in Table IIa the other, with outward motion, is listed in Table IIb.

We assume that a constant velocity correction will eliminate the orbital motion in each group, leaving range-rate as it would be seen from the Earth's center. We use the principles of least-squares to find the constants that minimize the squared residuals of the solutions for  $a$  and  $e$ . For the first group, the constant is  $-.08$  km/see; for the second,  $+.15$  km/see. Both constants reduce the absolute value of the velocities, a result that is consistent with the above assumption.

The corresponding semi-major axes and eccentricities are, for the observations in Table IIa,  $a = 9285 \pm 148$  km and  $e = .0204 \pm .0097$ . For Table IIb,  $a = 9405 \pm 116$  km and  $e = .0220 \pm .0070$ . There is good agreement between these values and we adopt the mean values  $a = 9345$  km and  $e = .0212$ .

From the average semi-major axis and the assumption of zero eccentricity, we can find from the data in figure 6 an estimate of the orbital precession for a single orbiting cluster. A straight line fitted to the three peaks gives a precession of  $+6.0 \pm .5$  hours per year, a value which corresponds to an inclination of  $95.5 \pm 1$  deg for the cluster.

**6b . Properties of known debris in the altitude range 2500 to 5000 km.**

In order to find a source for this debris, we have searched Molczan's (1997) very extensive catalogue of orbital elements of (almost) all satellites still in Earth orbit. The results are given in figure 7, where altitude is plotted against inclination. The dotted line represents the error bars, and accounts for the fact that the inclination calculation depends upon the altitude. Only one spacecraft is a reasonable source of the debris - Midas 4.

On October 21, 1961, the West Ford Project, using Midas 4, attempted to place 350 million copper needles into a 3500 by 3800 km, 96 degree inclination orbit, as a communication experiment. Each needle was 1.77 cm long and .00286 cm thick with an area to mass ratio of  $39.1 \text{ cm}^2 \text{ gi}^{-1}$ .

The orbit was carefully chosen so that an object of this area to mass ratio would reenter the Earth's atmosphere within 5 years due to perturbations caused by solar radiation pressure. However, rather than orbit as individual needles, they stuck together, splitting into smaller lumps from time to time. Because of their much smaller area to mass ratio, the lumps did not reenter as planned.

The West Ford Project attempted the experiment again in May, 1963. This time 400 million needles were launched, each 1.78 cm

long and .00178 cm thick, leading to an area to mass ratio of  $62.7 \text{ cm}^2 \text{ gi}^{-1}$ . This ratio required an orbit 3600 by 3700 km, 87 degree inclination for the needles to reenter within 5 years. This time, all but 1/3 of them stuck together, and the experiment was declared a success. Even though some authors have maintained that all of the needles have reentered, new lumps of needles continue to be cataloged over 30 years after the West Ford Project, Shapiro (1966), Martin (1967) and Gabbard (1970).

The putative dipoles were manufactured to be resonant at the same wavelength as the Goldstone transmitter - 3.5 cm. This is not such a coincidence as may seem; the Goldstone and West Ford transmitters have a common heritage. We calculate that the radar cross section of a West Ford dipole is  $265 \text{ mm}^2$  when its axis is perpendicular to the line of sight. Such an orientation is unstable, however, as the gravity gradient effect favors a vertical alignment, along the line of sight. Thus most measurements would yield radar cross sections well below the maximum. The radar cross sections of the West Ford dipoles would not depend on the sense of circular polarization.

Only 0.1% of the objects in one of the West Ford launches are required to obtain the 400,000 objects inferred from these observations. The fact that most of the objects were detected during a one hour interval of time suggests a recent release. If a lump of needles were to become unstuck (possibly by collisions with meteoroids of other needles) just prior to these observations, then the released needles would travel in a cluster similar to that observed. Solar radiation pressure would change the eccentricity of the individual needles, either increasing or decreasing the perigee altitude, depending on the orientation of their orbit when released. The needles would soon be undetectable, either because they were too high, or because they had reentered.

Barsukov and Nazarova (1988) have reported that the flux of micrometeorites observed from the Elektron 1 and 3 spacecraft was maximum in the altitude range 3000 to 3500 km. It seems unlikely that these much smaller particles are associated with the ones we have observed near 2900 km, but not impossible. Barsukov and Nazarova considered that they had observed meteoritic material in Earth orbit previously predicted at this altitude by Yu. G. Gulak.

Another possible source for the radar reflections are the hypothetical comets of Frank, Sigwarth and Craven (1986), based on observations of dark spots in the ultraviolet glow of Earth from a high-orbit Earth satellite.

## 7. Summary and Conclusions

We obtained additional measurements of the altitudes and cross sections of the material in the near cluster. We also made a statistical test of the polarization measurement at Haystack that confirms that there is much less power reflected when the

received sense of circular polarization is the same as the transmitted sense. Consequently, we help confirm the previous interpretation that spherical droplets from the RORSAT vehicles are the particles of the near cluster.

The distant cluster has particles with cross sections close to those expected for the West Ford dipoles. The lack of a statistical change in the reflected power when the polarization was inverted is that to be expected for dipoles. The inclination we found for the particle orbits agrees with only one spacecraft, that which launched the West Ford dipoles. Although the altitude of the distant cluster is slightly smaller than that of the spacecraft, solar pressure has the capability of changing the altitude of objects with such a small mass to area ratio.

It would be very unusual for meteoritic or cometary particles to have such a well-defined, low eccentricity orbit and an inclination of 96 deg.

Therefore, we conclude that the best explanation for the particles in the distant cluster is that they are West Ford dipoles from the 1961 launch. The long duration of these particles may be a result of delay in the dispersing device. An alternate possibility is that there exists a mechanism for adding energy to the orbiting dipoles.

### **Acknowledgements**

We thank the telescope operators at the Goldstone Tracking Station for their excellent support. The research described in this paper was carried out, in part, by the Jet Propulsion Laboratory, California Institute of Technology, under a contract with the National Aeronautics and Space Administration.

Table IIa  
October 17, 1994 observations

GMT (hours)	range (km)	velocity (km/see)
8.0956	2875.9	.1830
8.1044	2674.5	.0341
8.1594	2844.6	.0466
8.1825	3022.3	.2835
8.2022	2858.1	.1146
8.2181	2961.0	.1469
8.2378	2933.2	.2075
8.2467	2914.7	.2057
8.3019	2822.4	.0723
8.3181	2790.0	.0283
8.3475	2794.0	.0580
8.3581	2868.3	.1413
8.3819	2849.9	.1126
8.4222	2848.6	.1987
8.4364	2902.4	.1478
8.4706	2616.4	1231
8.4839	2760.7	-.1523
8.5181	2809.1	.0227
8.5389	2952.2	.2360
8.5583	2845.7	.0955
8.5608	2794.6	.0031
8.6133	3040.1	.2817
8.6189	2760.5	.0041
8.6472	2778.1	-.0048

Table IIb  
November 4, 1994 observations

GMT (hours)	range (km)	velocity (km/see)
7.8386	2892.1	-.1639
7.8781	2927.0	-.2523
7.8822	2905.1	-.0815
7.9136	2931.9	-.0109
7.9467	2923.4	-.1824
7.9586	2942.0	-.1068
7.9900	2917.3	-.2693
8.0647	2922.7	-.0439
8.1208	2889.6	-.0629
8.1450	2816.1	-.0840
8.1506	2926.7	-.0451
8.1800	2993.5	.0777
8.5983	2864.1	-.3488
8.6381	3044.0	.0125
8.8894	2883.5	-.0394
9.3064	2946.1	-.0913
9.5842	2919.6	-.0014
9.6286	2990.2	-.0051

## References

- Barsukov, V. L., and T. N. Nazarova, "Circular Dust Formations Around Earth and Moon and Some Structural Elements of Dust Formation around Sun", *Astronomicheskiy Vestnik*, pp 61-70, Jan.-Mar. , 1988.
- Frank, L. A., J. B. Sigwarth and J. D. Craven, "On the influx of small comets into the Earth's upper-atmosphere. 1. Observations", *Geophys. Res. L.*, Vol. 13, No. 4, pp. 303-306, 1986.
- Gabbard, John, "West Ford Needles - Launch 1963-14", NORAD 14EDC Memorandum for Record 70-141, June 30, 1970.
- Goldstein, R. M. and L. W. Randolph, "Rings of Earth", *IEEE Trans on Microwave Theory and Techniques*, Vol. 40, No. 6, Pp. 1077-1080, June, 1992.
- Goldstein, S. J. and R. M. Goldstein, "Some Properties of Millimetric Space Debris", *The Astronomical Journal*, Vol. 107, No. 4, pp. 367-371, Jan., 1994.
- Goldstein, R. M. and S. J. Goldstein, "Flux of Millimetric Space Debris", *The Astronomical Journal*, Vol. 110, No. 3, pp. 1392-1396, Sept., 1995.
- Johnson, N. L., "United States space Surveillance", *Advances in Space Research*, Vol. 13 (8), pp.5-20, Aug., 1993.
- Kessler, D. J., R. C. Reynolds and P. D. Anz-Meador, "Current Status of Orbital Debris Models", 33rd Aerospace Sciences Meeting and Exhibit, Reno NV, paper no. AIAA 95-0662, Jan. 9-12, 1995.
- Mandeville, J. C. and L. Berthaud, "From LDEF to EURECA - Orbital Debris and Meteoroids in Low-Earth Orbits", *Advances in Space Research*, Vol. 16 (11), pp.67-72, 1995.
- Martin, Charles-Noel, "Satellites into Orbit", pp 86-94, translated by T. Schoeters, published by George G. Harrap & Co., LTD, 1967.
- Molczan, Anonymous FTP:  
kilroy.jpl.nasa.gov/pub/space/elements/molczan
- Potter, A. E., "Ground-Based Optical Observations of Orbital Debris - A Review", *Advances in Space Research*, Vol. 16 (11), pp. 35-40, 1995.
- Shapiro, I. I., "Last of the West Ford Dipoles", *Science*, Vol. 154, no. 3755, pp. 1445-1448, Dec. 16, 1966.
- Stansbery, E. G., G. Bohannon, C. Pitts, T. Tracy and J. Stanley, "Radar Observations of Small Space Debris", *Advances in Space Research*, Vol. 13 (8), pp. 43-48, Aug., 1993.
- Stansbery, E. G., D. J. Kessler and M. J. Matney, "Recent results of Orbital Debris Measurements from the Haystack Radar", 33rd Aerospace Sciences Meeting and Exhibit, Reno, NV, paper no. AIAA 95-0662, Jan. 9-12, 1995.

## Figures

- 1) Location and beam intersection geometry of transmitting and receiving antennas.
- 2) Time-delay and time-of-day response for one space debris encounter, near the detection threshold.
- 3) Results of 38.4 hours of observations, effective diameter versus range.
- 4) Results, line-of-sight velocity versus range.
- 5) Measured flux of small particle space debris.
- 6) Histograms of arrival times for the distant cluster of debris.
- 7) Plot of Altitude versus Inclination of satellites now in Earth orbit. Only Midas 4 is close to the observations, indicating it is the source of the debris.

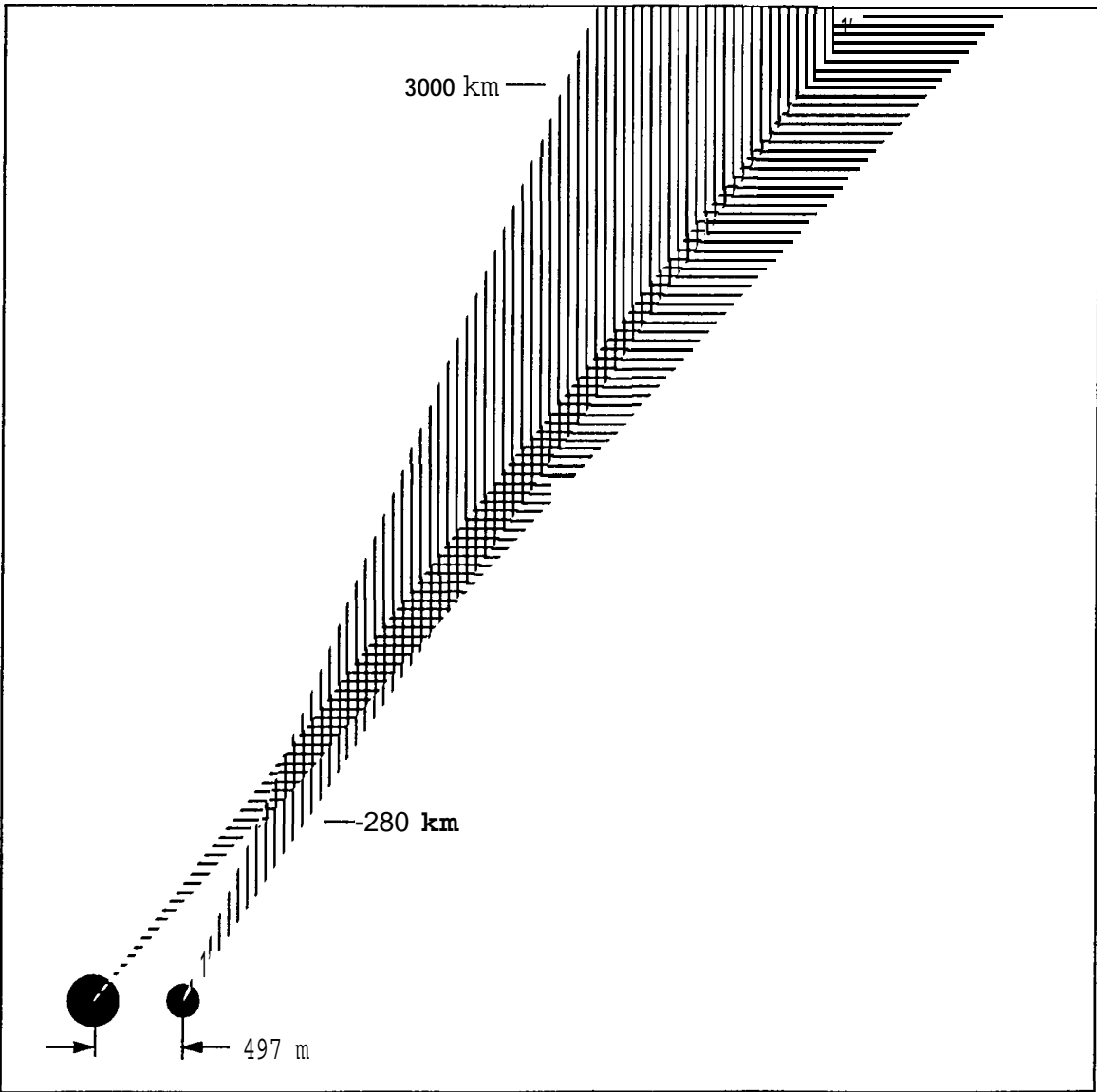
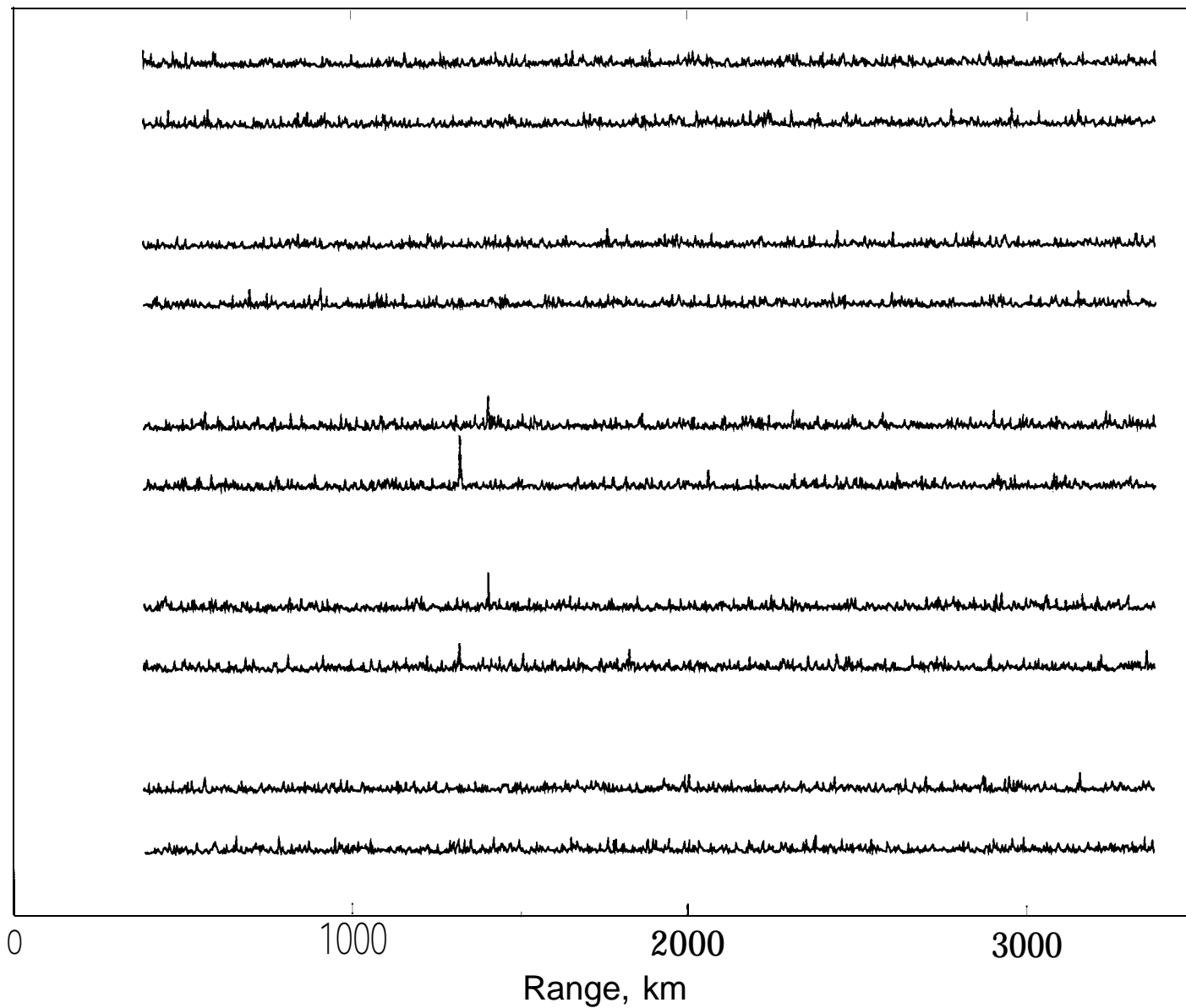


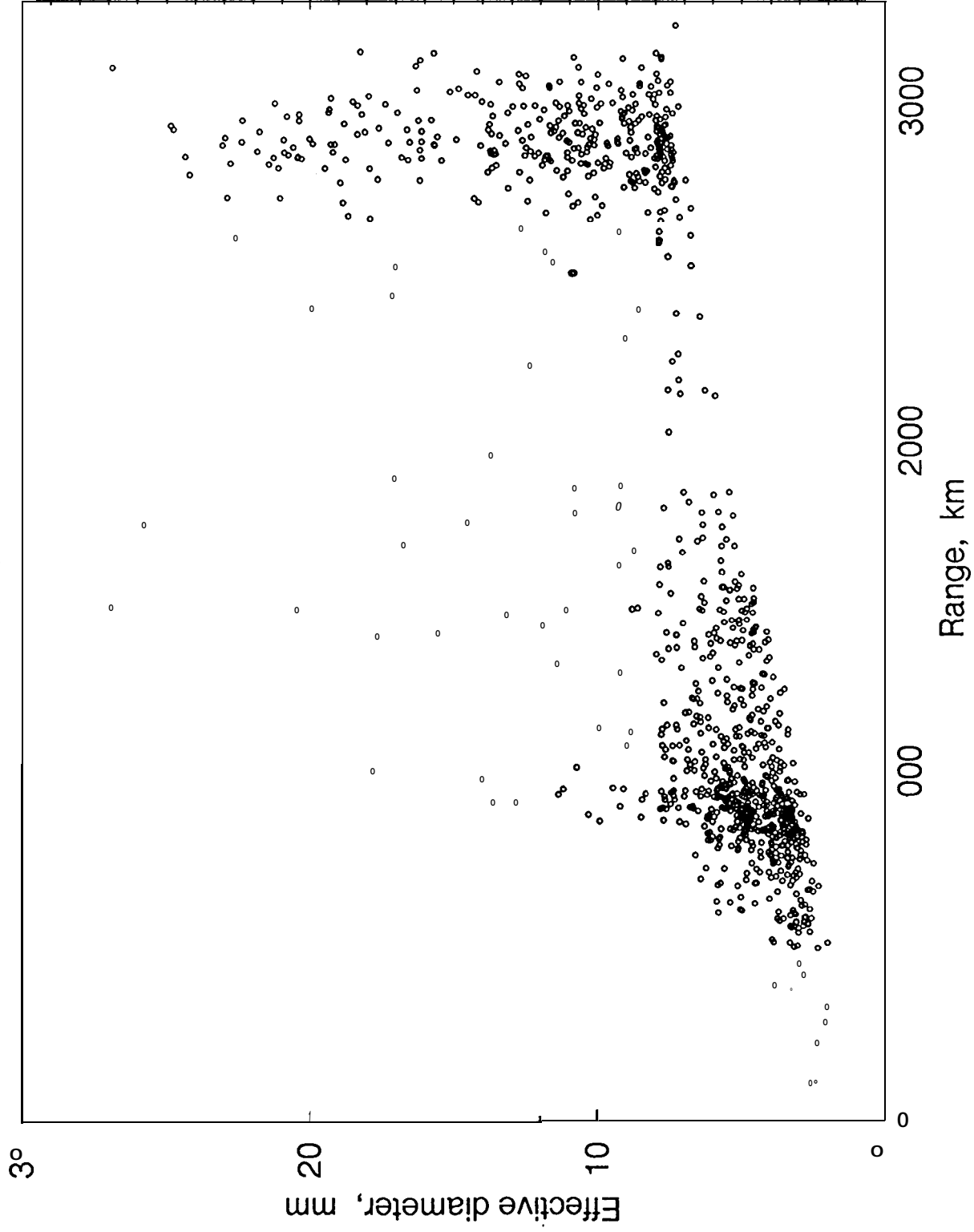
Figure 1

3/1 2/96 00:37:35



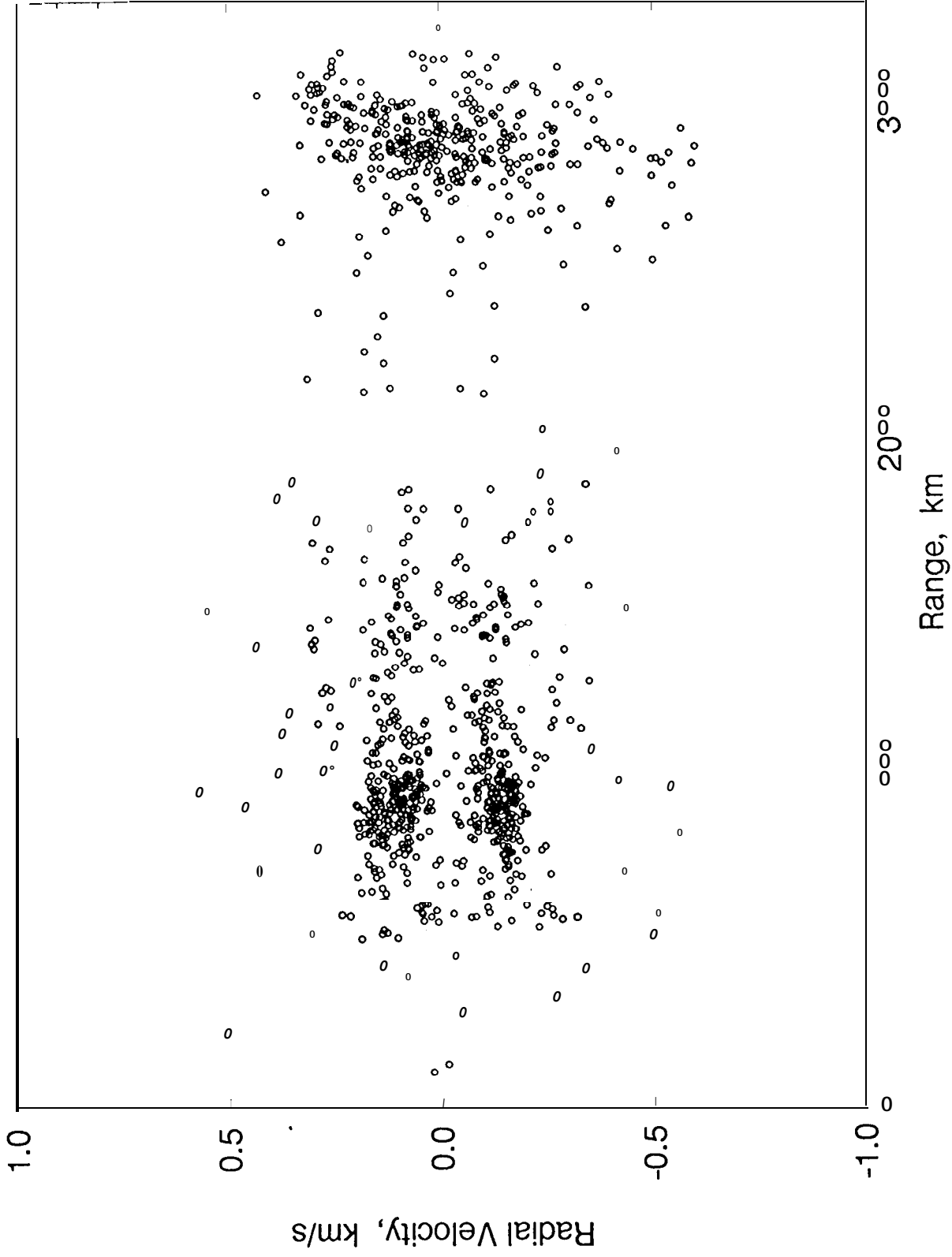
# Space Debris

Cumulative, 38.4 hours

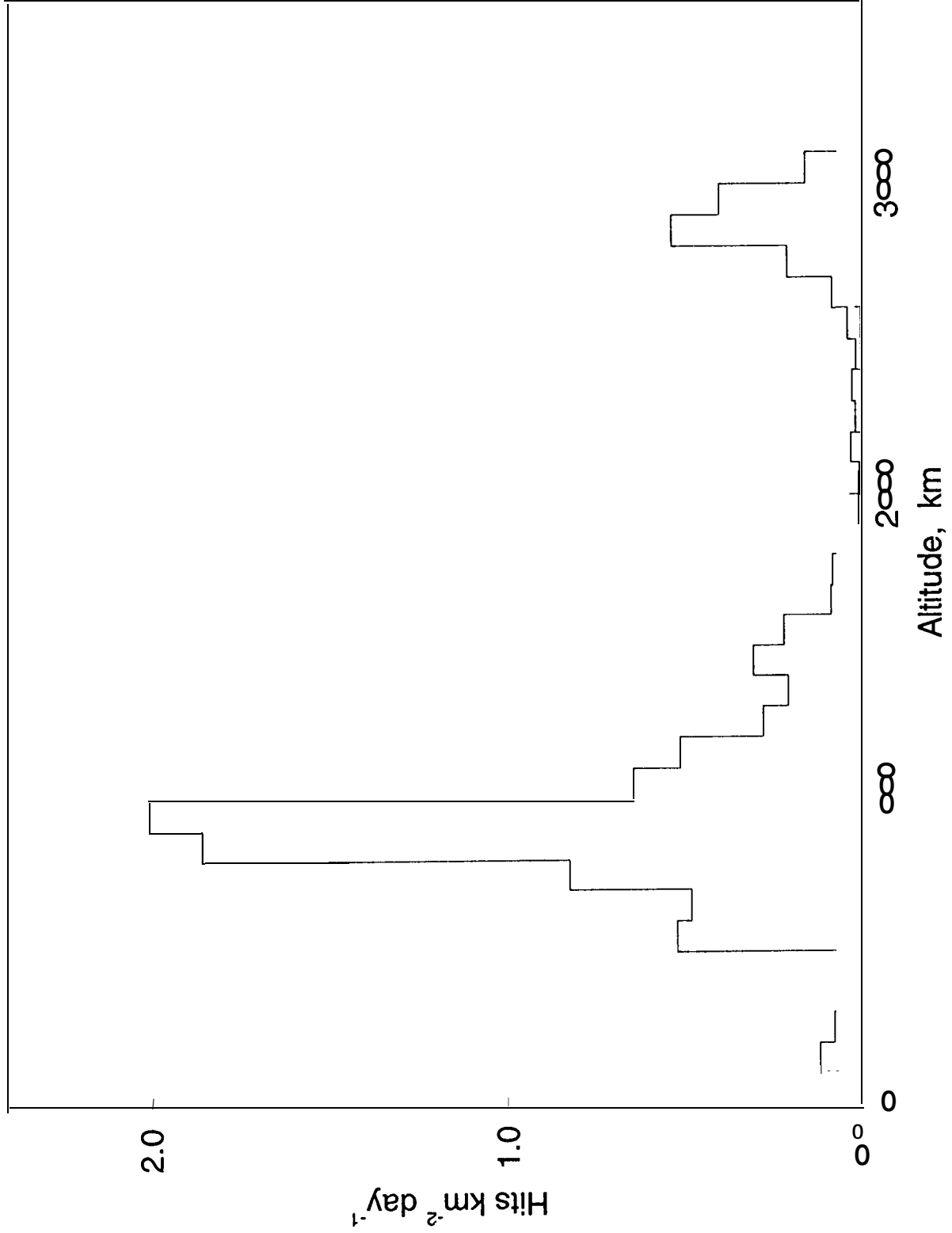


# Space Debris

Cumulative, 38.4 hours

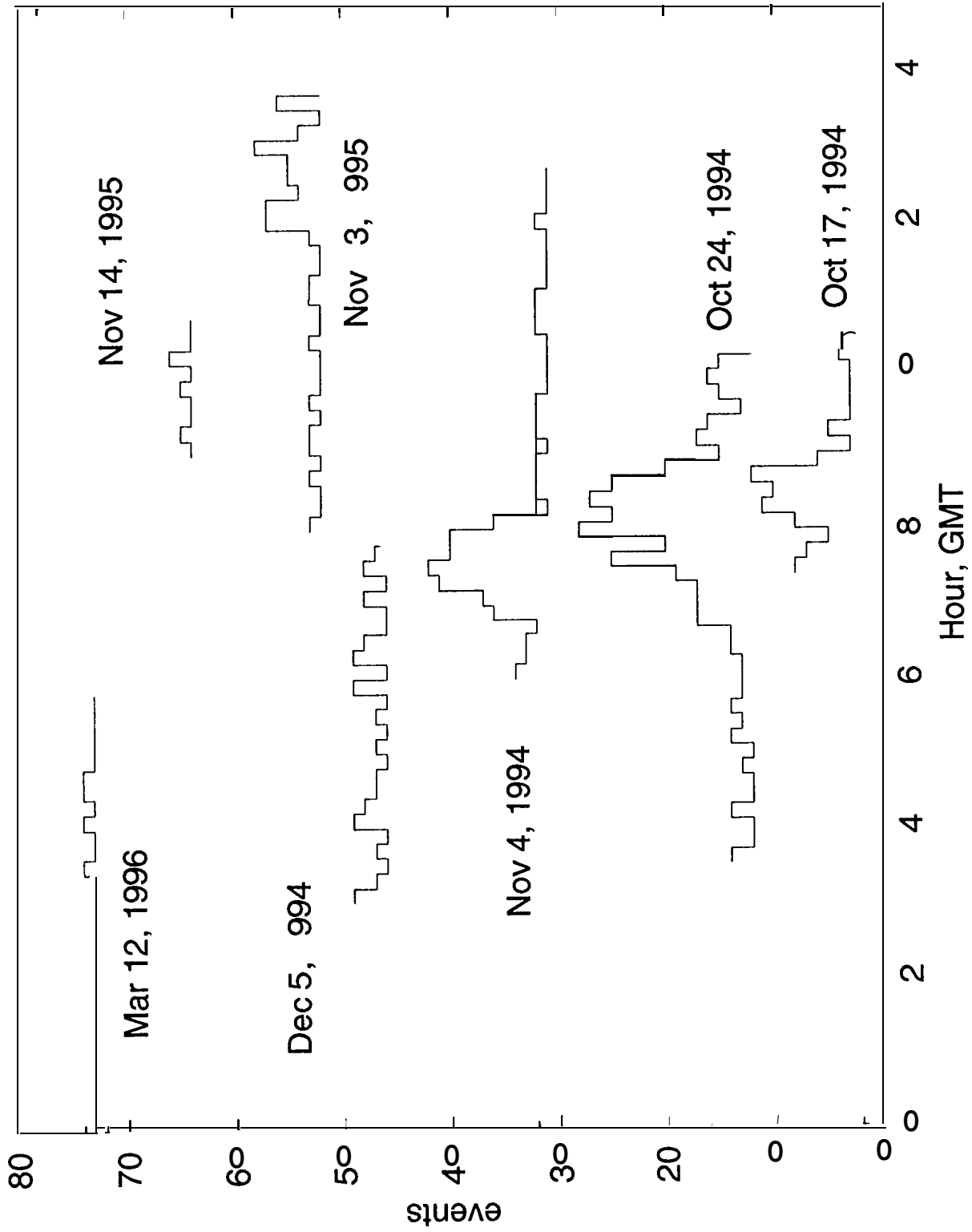


# Space Debris Flux



# Histograms

Distant Cluster



# Satellite Orbits

